



# Binary recycled pulsars: a powerful physical laboratory

G. Bisnovaty-Kogan

Space Research Institute Rus. Acad. Sci. Profsoyuznaya 84/32, 117997 Moscow, Russia  
e-mail: gkogan@iki.rssi.ru

**Abstract.** We discuss the problems of formation and evolution of pulsars in close binaries. The first discovered binary pulsar called Hulse-Taylor pulsar, on the name of discoverers. Observations indicate to existence of single recycled pulsars, and disruption of pulsar pairs. by the mechanism of enhanced evaporation is considered. The best laboratory of a study of General Relativity is a system of two neutron stars, where one, or two of them are radiopulsars. Hulse-Taylor pulsar, and recently discovered system containing two radiopulsars (a Double pulsar system) are the best objects for these studies. In addition to checking the validity of general relativity, these systems are used for putting limits to the variability of the gravitational constant. At the end the "Space Watch" device is described, which may permit to obtain the most precise universal time for the people on Earth.

**Key words.** Stars: neutron stars, radio pulsars, close binaries. General relativity.

## 1. Introduction

Discovery of pulsars was announced by Hewish et al. (1968). Until 1973 all known pulsars (more than 100) had been single, while more than half massive stars (predecessors of pulsars) are in binaries. Possible explanations of this fact had been suggested: all pairs are disrupted during explosion, or there is no possibility to form a radiopulsar, in pairs Trimble & Rees (1970).

## 2. Pulsars and close binaries

X-ray satellite UHURU was launched in 1970, and soon after that X-ray pulsars in binaries had been discovered. One of the best studied is X ray pulsar Her X-1. It has pulsation pe-

riod  $P_p \approx 1.24$  sec, orbital period  $P_{orb} \approx 1.7$  days, neutron star mass about  $1.4 M_\odot$ , and optical star with a mass about  $2M_\odot$ , see e.g Scott et al. (2000).

It was shown by Bisnovaty-Kogan & Komberg (1974), that this system should give birth to the binary radiopulsar, by following reasons. 1. After 100 million years the optical star will become a white dwarf, mass transfer will be finished, and the system will be transparent to radio emission. 2. X ray pulsar is accelerating its rotation due to accretion, so after the birth of the white dwarf, the neutron star will rotate rapidly, with  $P_p$  about 100 ms. It was suggested by Bisnovaty-Kogan & Komberg (1974), that binary radiopulsars had not been not found until 1973, because the magnetic field of the neutron star is decreasing about 100 times during the accretion, so binary

---

Send offprint requests to: G. Bisnovaty-Kogan

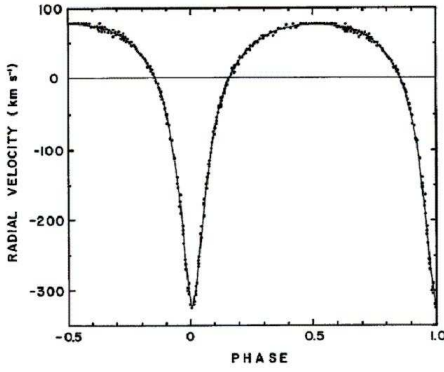


**Fig. 1.** Velocity curve for the first binary pulsar. Points represent measurements of the pulsar period distributed over parts of 10 different orbital periods. The curve corresponds to the pulsar parameters from the text.

radiopulsars are very faint objects. Pulsar luminosity  $L \sim B^2/P^4$ , so at small  $B$ , luminosity  $L$  is low even at the rapid rotation. Magnetic field is decreasing due to screening by the infalling plasma.

### 3. Hulse-Taylor pulsar

Hulse & Taylor (1975) had discovered the first binary radiopulsar with a period  $P_p = 0.05903$  s, orbital period  $P_{orb} \approx 7.75$  h, orbit eccentricity  $e = 0.615$  (see Fig.1). The properties of the first binary pulsar coincide with our predictions: rapid rotation together with a small magnetic field, Taylor et al. (1976), Bisnovatyi-Kogan & Komberg (1976)

$$\dot{E} = -I\Omega\dot{\Omega} = I \left( \frac{2\pi}{P_p} \right)^2 \frac{\dot{P}_p}{P_p} = 2 \cdot 10^{33} \text{ erg/s}, \quad (1)$$

$$B_p^2 = \left( \frac{3Ic^3 P_p \dot{P}_p}{8\pi^2 R_{NS}^6} \right)^{1/2} \approx 2.3 \cdot 10^{10} \text{ Gs.}$$

The average magnetic fields of single radiopulsars is about  $10^{12}$  Gauss.

### 4. Disrupted pulsar pairs

Suggestions for separation of pulsars at birth was done by Bisnovatyi-Kogan & Komberg

(1974) where 10 pairs of single pulsars with a possible origin from one pair had been listed (see Table 1). The same idea was recently considered by Vlemmings et al. (2005), who measured pulsar proper motions. They suggested a common origin of the pair B2020+28 and B2021+51. It is interesting, that one of this pulsars (2020+28) had been suggested by Bisnovatyi-Kogan & Komberg (1974) for the common origin with another pulsar (2016+28, line 8 in Table 1). The last pulsar is much closer to B2020+28 on the sky, and both are situated at the same distance, Lyne et al. (1998). The pulsar B2021+51 is much farther on the plane, and almost two times by the distance, but velocities intersect in Cygnus OB association.

### 5. Recycled pulsar (RP) statistics

Recycled pulsars is a separate class of neutron stars, containing more than 180 objects. All passed the stage of accreting pulsars, accelerating the rotation and decreasing the magnetic field. So we have ordinary pulsars with  $P_p = 0.033 - 8$  s,  $B = 10^{11} - 10^{13}$  Gs; and recycled pulsars with  $P_p = 1.5 - 50$  ms,  $B = 10^8 - 10^{10}$  Gs. These two groups are distinctly visible on the  $P - \dot{P}$  diagram (Fig.2).

### 6. Enhanced evaporation: formation of single RP

Most recycled pulsars consist of pairs NS + WD, and single NS, about 180 objects in total. Only 6 NS + NS pairs exist, like Hulse-Taylor pulsar. Single recycled pulsars (small  $P_p$  and  $B$ ) have passed the stage of X-ray pulsar in binary, and later had lost the WD companion. Besides, NS + NS are in the Galaxy disk, and NS + WD, and single are in the galactic bulge, and in the globular clusters. Globular clusters contain 0.001 of the mass of the Galaxy, and about 1/2 of the recycled pulsars. Formation of the binary in GC may happen by tidal capture or triple collision. Disruption of the binary RP also happens by collisions with GC stars: most single RP are situated in GC. In the most dense GC we have, according to Lorimer (2005), 31 RP in Terzian 5 (11 BP, 10 +10? single); 22

**Table 1.** Single pulsars of possible common origin, from Bisnovatyi-Kogan & Komberg (1974).

No	PSR	R. A.	Decl	$l''$	$b''$	$P_s$	DM $\frac{pc}{cm^3}$	$\dot{P} \frac{s}{day}$	$\tau = \frac{P}{\dot{P}} yr$
1	P0943+10	9 <sup>h</sup> 43 <sup>m</sup> 20 <sup>s</sup>	10°05'33''	225.4	43.2	1.098	15	-	-
	P0950+08	9 50 31	08 09 43	228.9	43.7	0.253	3	0.0198	3.5·10 <sup>7</sup>
2	P0809+74	8 09 03	74 38 10	140	31.6	1.30	6	0.014	2.5·10 <sup>8</sup>
	P0904+77	9 04	77 40	135.3	33.7	1.58	-	-	-
3	P1700-18	17 00 56	-18	4.0	14.0	0.802	≤40	0.154	6.9·10 <sup>6</sup>
	P1706-16	17 06 33	-16 37 21	5.8	13.7	0.653	25	0.55	3.3·10 <sup>6</sup>
4	P0329+54	3 29 11	54 24 38	145.0	-1.2	0.714	27	0.177	1.1·10 <sup>7</sup>
	P0355+54	3 55 00	54 13	148.1	0.9	0 156	55	-	-
5	P0525+21	5 25 45	21 55 32	183.8	-6.9	3.7455	51	3.452	3·10 <sup>6</sup>
	P0531+21	5 31 31	21 56 55	184.6	-5.8	0.03313	57	36.526	2.5·10 <sup>3</sup>
6	P1426-66	14 26 34	-66 09 94	312.3	-6.3	0.787	60	-	-
	P1449-65	14 49 22	-65	315.3	-5.3	0.180	90	-	-
7	P1845-01	18 45	-01 27	31.3	0.2	0.660	90	-	-
	P1845-04	18 45 10	-04 05 32	28.9	-1.0	0.598	142	-	-
8	P2016+28	20 16 00	28 30 31	68.1	-4.0	0.558	14.16	0.01	1.2·10 <sup>8</sup>
	P2020+28	20 20 33	28 44 30	68.9	-4.7	0.343	-	-	-
9	P2111+46	21 11 41	46 36	89.1	-1.2	1.015	141.4	-	-
	P2154+40	21 54 56	40 00	90.5	-11.5	1.525	110	-	-
10	P0611+22	06 11 10	22 35	188.7	2.4	0.335	99	-	-
	P0540+23	05 40 10	23 30	184.4	-3.3	0.246	72	-	-

RP in 47 Tuc (14 BP, 7 + 1? single). In total: 80 RP in Gal (15 single), 108 RP in GC (40+15? single).

Simple disruption of the pair by collisions with field stars does not work, because hard pairs become even harder by collisions. When pair is in a state of a disk accretion, with WD filling its Roche lobe (Fig.3) situation is opposite, and also hard pairs become softer during collisions due to enhanced mass transfer, and finally pair is disrupted. This process named "enhanced evaporation", first considered by Bisnovatyi-Kogan (1990), could explain formation of single RP in GC, and their appearance in bulge may be connected with a full evaporation of GC (see also Bisnovatyi-Kogan (2006)).

## 7. General relativity effects: NS+NS

In the NS+NS binary tidal effects are negligibly small, so several post-keplerian (PK) GR effects had been measured from pulsar timing. They include, according to Taylor (1994), the

parameter  $\dot{\omega}$ , determining the rate of relativistic apse line motion, the parameter  $\gamma$ , representing the amplitude of the signal time delay due to variable gravitational redshift and time dilation (quadratic Doppler effect), when the pulsar moves in an elliptical orbit. Emission of gravitational waves results in the loss of the orbital angular momentum and decreases the orbital period  $\dot{P}_{orb}$ . The parameters  $r$  and  $s$  determine the time delay due to the Shapiro effect and are related to the companion's gravitational field.

$$\dot{\omega} = 3T_{\odot}^{2/3} \left( \frac{P_{orb}}{2\pi} \right)^{-5/3} \frac{1}{1-e^2} (M_A + M_B)^{2/3}, \quad (2)$$

$$\gamma = T_{\odot}^{2/3} \left( \frac{P_{orb}}{2\pi} \right)^{1/3} e \frac{M_B(M_A + 2M_B)}{(M_A + M_B)^{4/3}}, \quad (3)$$

$$\dot{P}_{orb} = -\frac{192\pi}{5} T_{\odot}^{5/3} \left( \frac{P_{orb}}{2\pi} \right)^{-5/3} \quad (4)$$

$$\times \frac{\left(1 + \frac{73}{24}e^2 + \frac{37}{96}e^4\right)}{(1-e^2)^{7/2}} \frac{M_A M_B}{(M_A + M_B)^{1/3}},$$

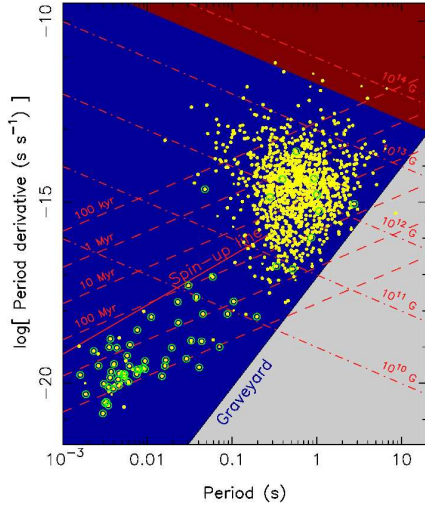


**Fig. 2.** The location of pulsars on the  $P-\dot{P}$  diagram (period-period derivative). Pulsars in binary systems are encircled, Lorimer (2005).

$$r = T_{\odot} M_B, \quad (5)$$

$$T_{\odot} = GM_{\odot}/c^3 = 4.925490947 \mu\text{s},$$

$$s = x T_{\odot}^{-1/3} \left( \frac{P_{orb}}{2\pi} \right)^{-2/3} \frac{(M_A + M_B)^{2/3}}{M_B}, \quad (6)$$

NS + NS RPs are the best laboratories for checking of General Relativity. 1913+16 timing had shown (indirectly) the existence of gravitational waves, Nobel Prize of Hulse and Taylor (1993)

## 8. A double pulsar system

A binary system, containing two pulsars with periods 23-ms (J0737-3039A), and 2.8-sec (B) was discovered in 2004 year by Lyne et al. (2004). This highly-relativistic double-neutron-star system allows unprecedented tests of fundamental gravitational physics. It was observed a short eclipse of J0737-3039A by J0737-3039B, and orbital modulation of the flux density and pulse shape of J0737-3039A, probably due to the influence of J0737-3039B energy flux upon its magnetosphere. These effects will allow to probe magneto-ionic properties of a pulsar magnetosphere. The obser-

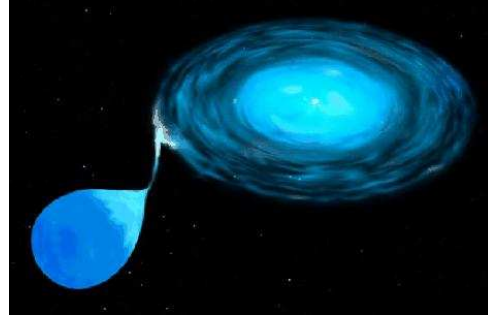


**Fig. 3.** Artistic vision of a disc accretion to the neutron star in X-ray sources (<http://antwrp.gsfc.nasa.gov/apod/ap991219.html>)

vatinal properties of this system are listed in Table.2, and artistic view is given in Fig.4.

## 9. Checking general relativity

Five equations in the system (2)-(6) contain two unknown masses. For correct gravitational theory all curves on the plane ( $M_A$ ,  $M_B$ ) intersect in the same point. Three curves available for the pulsar 1913+16 (Fig.5), and six curves for the double pulsar system (Fig.6, the additional line  $R$  follows from observations of both pulsars) intersect in one point inside the error limits, indicating the correctness of GR on the level  $\sim 0.4\%$  for 1913+16, after about 20 years of observations, and on the level  $\sim 0.1\%$  after one year of observations of the double system.

## 10. On the probability of gravitational wave registration from neutron star merging

As was shown by calculations of Kalogera et al. (2004) in the model of a pulsar evolution, the mean galactic merging rate of binary neutron star systems (BNS systems) is  $R \approx 83/\text{Myr}$ . The 68%- and 95%-confidence level intervals are 40 – 170 and 20 – 290 /Myr, respectively. The expected detection rate of a gravitational wave pulse from neighboring galaxies is 0.035 and 190 events per year for the initial (the detection limit 20 Mpc) and advanced (the detection limit 350 Mpc) LIGO interferometers, re-

spectively. The corresponding 95%-confidence intervals are 0.007 - 0.12 and 40 - 660 events per year, respectively. The discovery of the double pulsar J0737-3039 increased R by 6.4 times compared to earlier calculations, because it dominates in computing the total probability, as seen in Fig.7. Examination of a broader class of evolutionary models of pulsars showed that in all cases, accounting for the double pulsar J0737 - 3039 increases the BNS merging rate by 6 - 7 times, although the rates can differ by more than 50 times in individual cases

### 11. Variability of the gravitational constant.

Variations of the gravitational constant  $G$  have been measured by different methods, see Uzan (2003). The following restrictions are obtained from investigations of stellar and planetary orbits. Using of the Viking Lander ranging data gave limits  $\dot{G}/G = (2 \pm 4) \cdot 10^{-12} \text{yr}^{-1}$ . Anderson et al. (1992) have found, from the combination of Mariner 10 and Mercury and Venus ranging data, the following restriction

$$\dot{G}/G = (0 \pm 2) \cdot 10^{-12} \text{yr}^{-1}, \quad (7)$$

Lunar Laser Ranging experiments (LLR) are lasting for many years, and improve the estimations of  $\dot{G}/G$  from  $\dot{G}/G < 6 \cdot 10^{-12} \text{yr}^{-1}$  by Dickey et al. (1994), up to  $\dot{G}/G [\text{yr}^{-1}] = (6 \pm 8) \cdot 10^{-13}$  by Mueller et al. (2005). Incompletely modeled solid Earth tides, ocean loading or geocenter motion, and uncertainties in values of fixed model parameters have to be considered in those estimations.

Recycled pulsars give now the best available timing precision. The observed changes in the binary period of PSR B1913+16 coincide within the error bars with GR prediction of emission of gravitational waves. Measurements of the variations of the binary period give restrictions to the variation of the gravitational constant. Change of  $G$  has influence on the orbital motion, and only emission of the gravitational waves compete here with the variation of  $G$ . If we accept the correctness of GR, than we can use residuals (error box) of the measurements of decay of the binary period  $\dot{P}_b$  for the estimation of variations

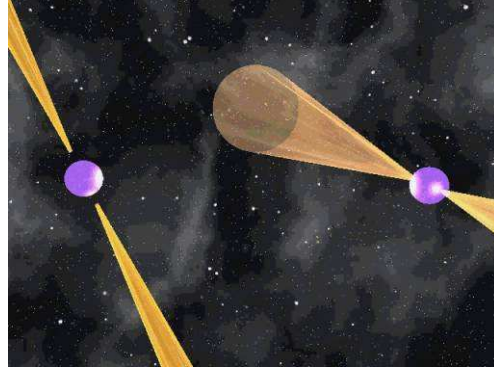


**Fig. 4.** Artistic picture of the double pulsar system, from Arons (2005).

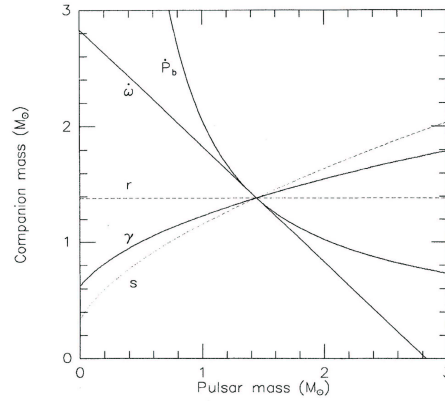


**Fig. 5.** Observational constraints on the component masses in the binary pulsar PSR 1913 + 16. The solid curves correspond to Eqns (2)-(4) with measured values of  $\dot{\omega}$ ,  $\gamma$ , and  $\dot{P}_{orb}$ . The intersection of these curves at one point (within an experimental uncertainty of about 0.35% in  $\dot{P}_{orb}$ ) proves the existence of gravitational waves. The dashed lines correspond to the predicted values of the parameters  $r$  and  $s$ . These values can be measured by future accumulation of observational data Taylor (1994).

of  $G$ , see Damour et al. (1988). It was obtained by Kaspi et al. (1994), using timing data from Taylor (1993)

$$\frac{\dot{G}}{G} = -\frac{1}{2} \frac{\dot{P}_b}{P_b} = (4 \pm 5) \cdot 10^{-12} \text{yr}^{-1}. \quad (8)$$

For the pulsar PSR B1913+16 the error budget for the orbital period derivative, in compar-

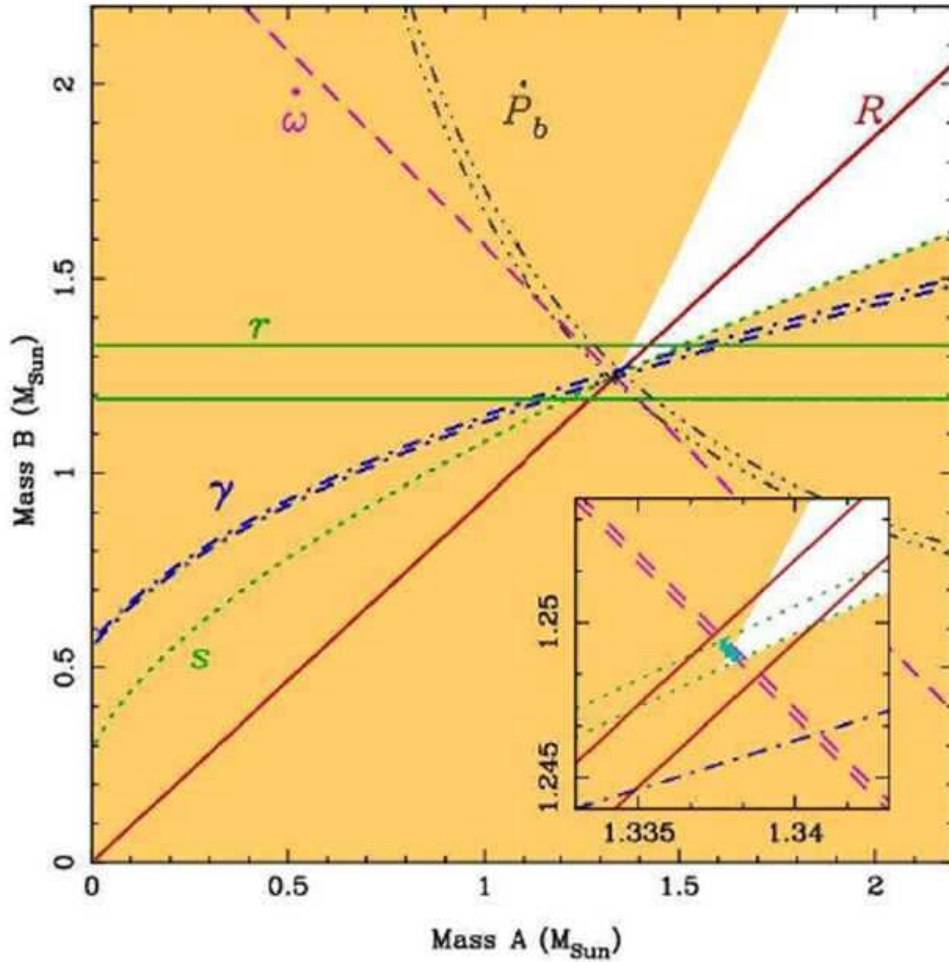


**Fig. 6.** The observational constraints upon the masses  $m_A$  and  $m_B$  in the double pulsar system J0737–3039. The colored regions are those which are excluded by the Keplerian mass functions of the two pulsars. Further constraints are shown as pairs of lines enclosing permitted regions as predicted by general relativity: (a) the measurement of the advance of periastron, giving the total mass  $m_A + m_B = 2.588 \pm 0.001 M_{\text{Sun}}$  (dashed line); (b) the measurement of  $R = m_A/m_B = 1.071 \pm 0.001$  (solid line); (c) the measurement of the gravitational redshift/time dilation parameter (dot-dash line); (d) the measurement of Shapiro parameter  $r$  (dot-dot-dot-dash line) and (e) Shapiro parameter  $s$  (dotted line). Inset is an enlarged view of the small square encompassing the intersection of these constraints, from Kramer et al. (2006).

ison with GR prediction, is given in Table 3, from Taylor (1993). Supposing that all deviations from GR are connected with  $G$  variation, it was obtained by Bisnovaty-Kogan (2006) the following upper limit for this variation:  $\frac{\dot{G}}{G} = (4.3 \pm 4.9) \cdot 10^{-12} \text{ yr}^{-1}$ .

These estimations slightly improve the values of Kaspi et al. (1994). This improvement narrows on 40% the boundary in the negative region, most important from the theoretical point of view. Combination the last result with the result of Anderson et al. (1992) per-

**Table 2.** Observed and derived parameters of PSRs J0737–3039A and B. Standard errors are given in parentheses after the values and are in units of the least significant digit(s). The distance is estimated from the dispersion measure and a model for the interstellar free electron distribution, from Lyne et al. (2004), Kramer et al. (2005).

Pulsar	PSR J0737–3039A	PSR J0737–3039B
Pulse period $P$ (ms)	22.699378556138(2)	2773.4607474(4)
Period derivative $\dot{P}$	$1.7596(2) \times 10^{-18}$	$0.88(13) \times 10^{-15}$
Right ascension $\alpha$ (J2000)	07 <sup>h</sup> 37 <sup>m</sup> 51 <sup>s</sup> .24795(2)	
Declination $\delta$ (J2000)	–30°39′40″.7247(6)	
Orbital period $P_b$ (day)	0.1022515628(2)	
Eccentricity $e$	0.087778(2)	
Advance of periastron $\dot{\omega}$ (deg yr <sup>–1</sup> )	16.900(2)	
Projected semi-major axis $x = asini/c$ (sec)	1.415032(2)	1.513(4)
Gravitational redshift parameter $\gamma$ (ms)	0.39(2)	
Shapiro delay parameter $s = \sin i$	0.9995(4)	
Shapiro delay parameter $r$ ( $\mu$ s)	6.2(6)	
Orbital decay $\dot{P}_b$ ( $10^{-12}$ )	–1.20(8)	
Mass ratio $R = M_A/M_B$	1.071(1)	
Characteristic age $\tau$ (My)	210	50
Surface magnetic field strength $B$ (Gauss)	$6.3 \times 10^9$	$1.6 \times 10^{12}$
Spin-down luminosity $\dot{E}$ (erg/s)	$5800 \times 10^{30}$	$1.6 \times 10^{30}$
Distance (kpc)	~0.6	

mits to narrow the range of  $G$  variations, which is now, according to Bisnovatyi-Kogan (2006), may be situated in the limits

$\dot{G}/G$  is within the interval  $(-0.6, 2) \cdot 10^{-12} \text{yr}^{-1}$ .

## 12. MATRE: Most Accurate Time measurements by REcycled pulsars (Space Watch)

Exact time measurements are needed in many branches of human activity, as well as by simple pedestrians. The nature had prepared us the most accurate available watch in the form of Recycled Pulsars. The precision of the period of these pulsars is very high, and they are changing their periods with time incredibly slowly:  $dP/dt = 10^{-19.5}$  for PSR 1953+29,  $P=6.133$  ms;  $dP/dt = 10^{-19.0}$  for PSR 1937+21,  $P=1.558$  ms, what is, for a long time period, much better than the highest available precision based on the hydrogen frequency standard.

I suggest to build the international time watch system based on radio observations of several most stable recycled pulsars. To build this system the following components should be constructed (see ?).

1. Several radio telescopes over the Earth, which provide stable continuous observations of the chosen pulsar(s) during 24 hours, and retransmission of the signal to the Earth satellites.
2. System of the Earth satellites (20-25) which accept the exact time signals from the radio telescopes, and retransmit them to the Earth, covering all the Earth surface, similar to GPS system.
3. Device which accept the exact time signal from the satellite, and give the exact local/universal time information (should be widely available, could be combined with the cell phone, or GPS device).
4. Software/hardware for transformation of the pulsar signal into the signal of the exact

**Table 3.** Error budget for the orbital period derivative, in comparison with the general relativistic prediction.

	Parameter	( $10^{-12}$ )
Observed value	$\dot{P}_b^{obs}$	$-2.4225 \pm 0.0056$
Galactic contribution	$\dot{P}_b^{gal}$	$-0.0124 \pm 0.0064$
Intrinsic orbital period decay	$\dot{P}_b^{obs} - \dot{P}_b^{gal}$	$-2.4101 \pm 0.0085$
General relativistic prediction	$\dot{P}_b^{GR}$	$-2.4025 \pm 0.0001$

time measurement on the radio telescopes, satellites, and in every receiving device.

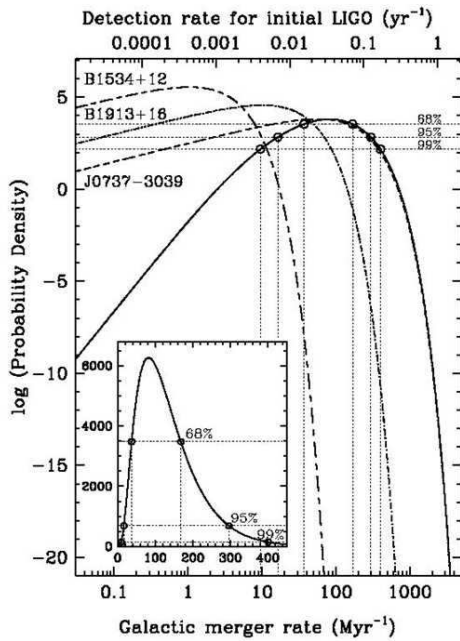


**Fig. 7.** Probability density function that represents our expectation that the actual DNS binary merger rate in the Galaxy (bottom axis) and the predicted initial LIGO rate (top axis) take on particular values, given the observations. The solid line shows the total probability density along with those obtained for each of the three binary systems (dashed lines). Inset: Total probability density, and corresponding 68%, 95%, and 99% confidence limits, shown in a linear scale, Kalogera et al. (2004).

Such system could be used in all branches of the human activity, including ordinary citizen. It should be really international, because its work depends on the synchronous and non-interruptive work of all telescopes in different countries. The cost of the construction of this system should be quite moderate (comparable with the construction of GPS), but the exact time is needed in much more wide cases than exact coordinates, simply because overwhelming majority of people have permanent place of life, or are moving along the well known routes. But watches are used by all of them. Therefore, this system could be quite profitable with time, because after construction it needs not much for supporting its work.

### 13. Conclusions

1. Timing of the pulsars J0737-3039A/B is the most powerful instrument for the verification of General Relativity due to unprecedented precision of the observations.
2. Recycled pulsars are the most precise available time standards.
3. Checking the physics beyond the standard: G-variability is possible by timing of recycled pulsars in close binaries.
4. The service of the exact time based on continuous observations of recycled pulsars may be constructed and used by pedestrians.

### 14. DISCUSSION

**RICHARD CONN HENRY:** Do I understand correctly that the limiting factor now in check-



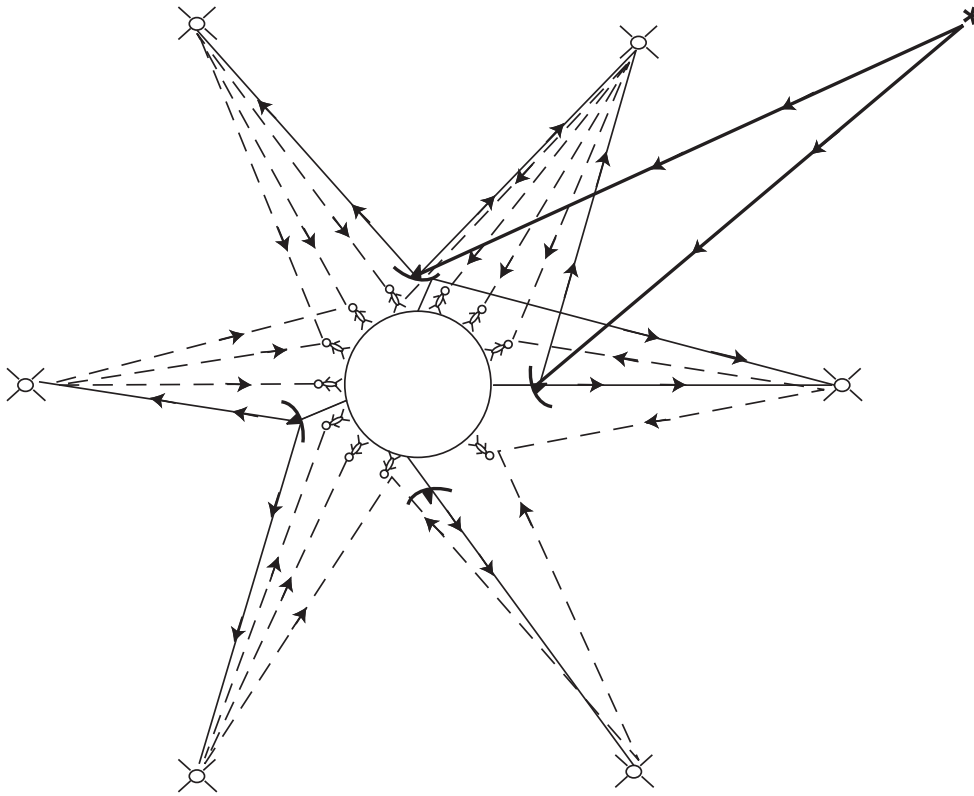


**Fig. 8.** Schematic sketch of the Space Watch system. The signal from the recycled pulsar (upper left) is accepted by the Earth radio telescopes, which transfer it to the satellite system. The pedestrians accept the exact time signal from the satellite by receivers similar to those used in GPS (or GLONASS).

ing the General Relativity is not the observations, but the second order calculations?

**GENNADY BISNOVATYI-KOGAN:** To extract second order GR effects, the precision of observations should be considerably improved. So while the calculations are really not simple, the observational progress seems to be even more important.

**WOLFGANG KUNDT:** Gennady, how do you solve the problem of the missing progenitors (of the supposed "recycled pulsars")?

**GENNADY BISNOVATYI-KOGAN:** The progenitors of the recycled pulsars are known

as low mass X-binaries, in some of which the millisecond X-ray pulsars had been observed.

**T. BULIK:** The coalescence rate increase due to discovery of J0737 is misleading. Within the errors the rate could also decrease even at the  $2\sigma$  level.

**GENNADY BISNOVATYI-KOGAN:** It is true that the error bars are very big, but the increase of the rate is related to the average value of this parameter.

**A. ZDZIARSKI:** Evolutionary scenario for the double pulsar.

**GENNADY BISNOVATYI-KOGAN:** Such scenario had been considered by many authors,

starting from A. Tutukov, L. Yungelson, E. van den Heuvel; see also Bisnovatyi-Kogan & Komberg (1974).

*Acknowledgements.* The author is grateful to F. Giovannelli, and other organizers of the workshop for support and hospitality. This work was partially supported by RFBR grants 08-02-00491, 08-02-90106, and President grant for a support of leading scientific schools 2977.2008.2.

## References

- Anderson, J.D., Armstrong, J.W., Campbell, J.K. et al. 1992, *Space Science Reviews* 60, 591
- Arons, J. 2005, *talk on KITP Program "Physics of Astrophysical Outflows and Accretion Disks"*, Apr 4 - Jul 29
- Bisnovatyi-Kogan, G.S. 1990, *Astrofizika* 32, 313
- Bisnovatyi-Kogan, G.S. 2006, *Phys-Usp* 49, 53
- Bisnovatyi-Kogan, G.S. 2006, *Int. J. Mod. Phys. D* 15, 1047
- Bisnovatyi-Kogan, G.S., Komberg, B.V. 1974, *Astron. Zh.* 51, 373
- Bisnovatyi-Kogan, G.S., Komberg, B.V. 1976, *Sov. Astr. L.* 2, 130
- Damour, T., Gibbons, G.W., Taylor, J.H. 1988, *PRL* 61, 1151
- Dickey, J.O., Bender, P.L., Faller, J.E. et al. 1994, *Science* 265, 482
- Hewish, A. Bell, S.J., Pilkington, J.D., et al. 1968, *Nature* 217, 709
- Hulse, R.A., Taylor, J.H. 1975, *Astrophys. J. Lett.* 195, L51
- Kalogera V. et al. 2004, *Astrophys. J. Lett.* 601, L179; 614, L137
- Kaspi, V.M., Taylor, J.H., Ryba, M.F. 1994, *ApJ* 428, 713
- Kramer, M., Lorimer, D.R., Lyne, A.G. et al. 2005, [astro-ph/0503386](https://arxiv.org/abs/astro-ph/0503386)
- Kramer, M., et al. 2006, [arXiv:astro-ph/0609417](https://arxiv.org/abs/astro-ph/0609417)
- Lyne, A.G., Graham-Smith, F. 1998, *Pulsar Astronomy* (Cambridge Univ. Press, UK)
- Lyne, A.G., Burgay, M., Kramer, M. et al. 2004, *Science* 303, 1153
- Lorimer, D.R. 2005, *Living Rev. Rel.* 8, 7; [astro-ph/0511258](https://arxiv.org/abs/astro-ph/0511258)
- Mueller, J., Williams, J.G., Turyshev, S.G. 2005, [gr-qc/0509114](https://arxiv.org/abs/gr-qc/0509114)
- Scott, D.M., Leahy, D.A. Wilson, R.B. 2000, *ApJ* 539, 392
- Taylor, J.H. 1993, *Classical and Quantum Gravity* 10, 167
- Taylor, J.H., Jr. 1994, *Reviews of Modern Physics* 66, 711
- Taylor, J.H., Hulse, R.A., Fowler, L.A., et al. 1976, *ApJL* 206, L53
- Trimble, V., Rees, M. 1970, in: *The Crab Nebula*. Proc. IAU Symp. 46. Eds. R. D. Davies and F. Graham-Smith. Dordrecht, Reidel, p.273 (1970).
- Uzan, J.-Ph. 2003, *Reviews of Modern Physics* 75, 403
- Vlemmings, W.H.T. et al. 2005, *Mem. Soc. Astron. It.* 76, 531